ARTICLE

BIOTECHNOLOGY and BIOENGINEERING

Metabolic Engineering of *Methanosarcina acetivorans* for Lactate Production From Methane

Michael J. McAnulty,[1] Venkata Giridhar Poosarla,[1] Jine Li,[1] Valerie W. C. Soo,[1] Fayin Zhu,[1] Thomas K. Wood[1,2]

[1]Department of Chemical Engineering, The Pennsylvania State University, University Park, Pennsylvania 168020-4400; telephone: +1 (814)-863-4811; fax: +1 (814)-865-7846; e-mail: tuw14@psu.edu

[2]Department of Biochemistry and Molecular Biology, The Pennsylvania State University, University Park, Pennsylvania 16802-4400

ABSTRACT: We previously demonstrated anaerobic conversion of the greenhouse gas methane into acetate using an engineered archaeon that produces methyl-coenzyme M reductase (Mcr) from unculturable microorganisms from a microbial mat in the Black Sea to create the first culturable prokaryote that reverses methanogenesis and grows anaerobically on methane. In this work, we further engineered the same host with the goal of converting methane into butanol. Instead, we discovered a process for converting methane to a secreted valuable product, *L*-lactate, with sufficient optical purity for synthesizing the biodegradable plastic poly-lactic acid. We determined that the 3-hydroxybutyryl-CoA dehydrogenase (Hbd) from *Clostridium acetobutylicum* is responsible for lactate production. This work demonstrates the first metabolic engineering of a methanogen with a synthetic pathway; in effect, we produce a novel product (lactate) from a novel substrate (methane) by cloning the three genes for Mcr and one for Hbd. We further demonstrate the utility of anaerobic methane conversion with an increased lactate yield compared to aerobic methane conversion to lactate.

Biotechnol. Bioeng. 2016;9999: 1–10.

KEYWORDS: metabolic engineering; anaerobic oxidation of methane; lactic acid

Background

Methane trapped in shale deposits has gained considerable attention as an energy source over the past decade in the United States since it decreases carbon dioxide emissions per unit energy consumed (Howarth, 2015). Methane, however, is a potent greenhouse gas that is 38-fold more effective at promoting global warming than carbon dioxide on a molar basis over a span of 20 years (Howarth et al., 2011; Shindell et al., 2009). Leaks of methane into the atmosphere commonly occur during procedures for extraction and transportation, distribution, and storage, with as much as an estimated 8% of the methane produced from a well leaking; of this, up to 4% are attributed to downstream processes of transportation, distribution, and storage (Howarth et al., 2011). Also, chemical processes for methane conversion (i.e., the Fischer–Tropsch process) are well established, but they require large initial capital investments (up to $20B) compared to potential biological processes that could be employed (Haynes and Gonzalez, 2014). Hence, to reduce leaks (from transportation, distribution, and storage) and capital cost, it is advantageous to convert methane biologically into a non-gaseous product at the site. Furthermore, harnessing methane is one of the most important near-term goals for biochemical engineering (Lee and Kim, 2015).

Among biological processes, anaerobic processes have higher carbon yields of potentially valuable products and energy efficiency compared to aerobic processes (Haynes and Gonzalez, 2014). Anaerobic oxidation of methane (AOM) that occurs in nature via anaerobic methanotrophic archaea (ANME) plays a large role in curtailing methane emissions, with an estimated 75 Tg methane per year captured by AOM; hence, 88% of the leaking methane from natural sources in the ocean is consumed before reaching the ocean surface (Reeburgh, 2007). Little is known about AOM, since no naturally-occurring individual species of ANME have been isolated that participate in AOM (Knittel and Boetius, 2009). Metabolic engineering strategies for conversion of methane to other products remain difficult as long as no individual species that perform AOM are isolated. However, we (Soo et al., 2016) recently reversed methanogenesis to achieve anaerobic growth on methane and bicarbonate and the production of acetate by the methanogen *Methanosarcina acetivorans* via heterologous expression of the methyl-coenzyme M reductase (Mcr) isolated from unculturable ANME from a microbial mat in the Black Sea (Shima et al., 2012). This activation of methane by a single species creates possibilities

Correspondence to: T.K. Wood

Contract grant sponsor: Department of Energy Advanced Research Projects Agency—Energy

Received 25 July 2016; Revision received 13 October 2016; Accepted 25 October 2016

Accepted manuscript online xx Month 2016;

Article first published online in Wiley Online Library (wileyonlinelibrary.com).

DOI 10.1002/bit.26208

for metabolic engineering for anaerobic methane conversion to other products (Soo et al., 2016).

The acetate produced by reversing methanogenesis may be converted to myriad products (Gajda et al., 2015; Hollinshead et al., 2014; Skjanes et al., 2008), including biofuels such as butanol (Gao et al., 2015). Butanol has great potential as a biofuel, since pure butanol can be used in a conventional ignition spark combustion engine (Wei et al., 2016). High titres (30 g/L) of butanol have been produced via acetyl-CoA in metabolically-engineered *Escherichia coli* (Shen et al., 2011); the pathway includes production of crotonase (Crt), 3-hydroxybutyryl-CoA dehydrogenase (Hbd), and aldehyde/alcohol dehydrogenase (AdhE2) from *C. acetobutylicum*, as well as production of trans-enoyl-CoA reductase Ter from Treponema denticola, and production of acetyl-CoA acetyltransferase (AtoB) from *E. coli* (Fig. 1). We reasoned butanol could be produced in an archaeal host with the same pathway if we substituted AtoB from *E. coli* with the putative acetyl-CoA acetyltransferase MA_4042 from *M. acetivorans* (UniProt Consortium, 2015). While attempting to convert methane to butanol in this work, unexpectedly, methane was converted into another valuable product, lactic acid (Fig. 1).

Lactic acid has a wide variety of uses in cosmetics, foods, and pharmaceuticals (Wee et al., 2006). For cosmetics, lactic acid is used as a skin exfoliant and humectant to reduce wrinkles and improve skin firmness and thickness (Smith, 1996). For foods, lactic acid is a generally recognized as safe food additive used to preserve olives, sauerkraut, and pickled vegetables, and it is used as an acidulant, flavoring, and pH buffering agent or inhibitor of bacterial spoilage in a wide variety of other processed foods (Datta et al., 1995). For pharmaceuticals, lactic acid has use in mineral preparations, drug delivery systems, and as an electrolyte in many parenteral and intravenous solutions (Wee et al., 2006). In addition, some lactic acid esters derived from lactate are environmentally-friendly (biologically derived and biodegradable)

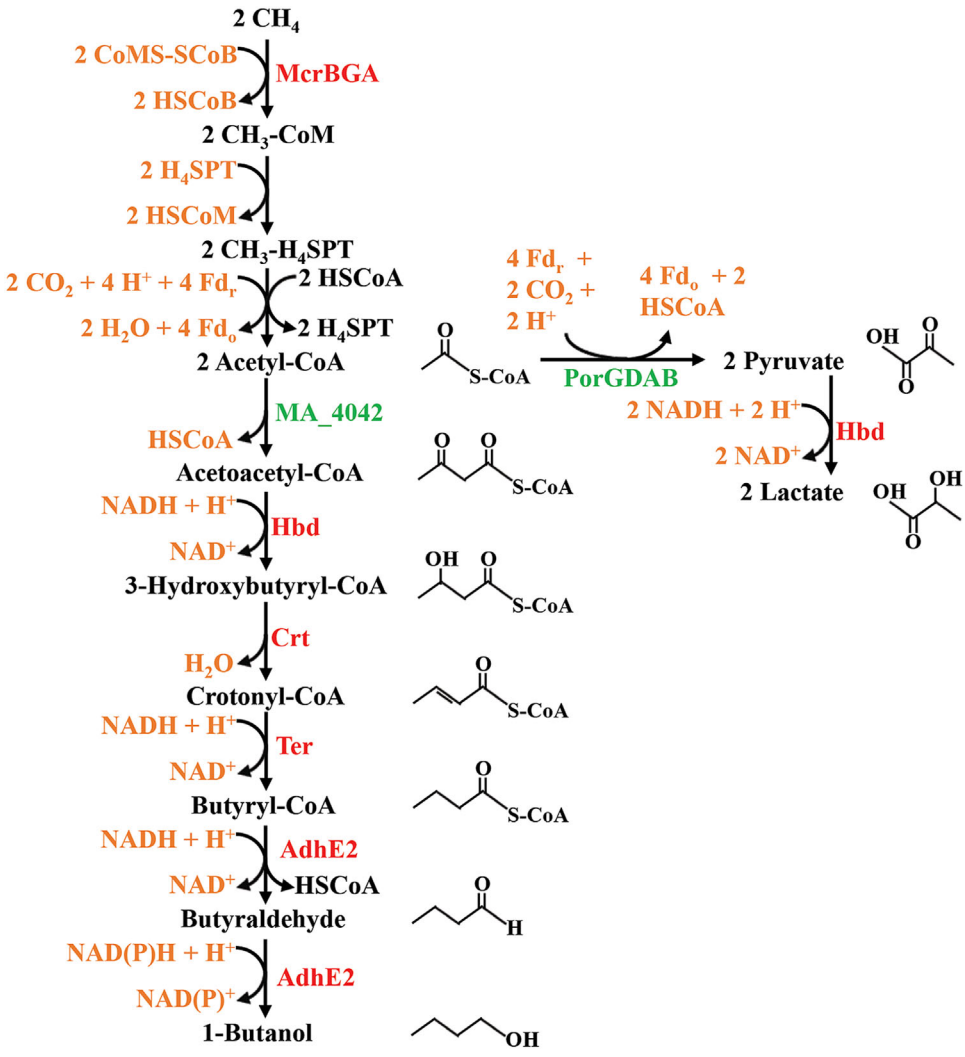

Fig. 1. Metabolic pathways for butanol and lactate production from methane. Enzymes produced from the plasmids used in this study are listed alongside their respective enzymatic step (those in red are heterologous and those in green are from the *M. acetivorans* host). The chemical structure of each intermediate is shown alongside the chemical name.

solvents that could replace more toxic ones currently in use (Corma et al., 2007), and others have hygroscopic and emulsifying properties applicable in the food, pharmaceutical, and cosmetic industries (Gao et al., 2011). Critically, lactic acid is likely to see increasing demand due to its use as a feedstock for producing the bio-degradable plastic poly-lactic acid (Upadhyaya et al., 2014). Optical purity (pure *D*- or *L*- lactate) is a prerequisite for the synthesis of poly-lactic acid of suitable quality for use as a plastic, since polymers consisting of both *D*- and *L*- lactic acid units may be amorphous and non-crystalline (Bogaert and Coszach, 2000). Synthetic routes for lactate production (mainly involving the hydrolysis of lactonitrile) result in racemic mixtures (Hofvendahl and Hahn-Hagerdal, 2000) unsuitable for poly-lactic acid synthesis, while biological methods can select specifically for *D*- or *L*- lactate production.

Heterologous expression of one enzyme has been utilized in an obligate aerobic methanotrophic host to produce lactate from methane, but yields were low at 0.06 g lactate/g methane (Henard et al., 2016). We reasoned that converting the process to an anaerobic host may improve the overall yield for lactate as suggested for the conversion of methane to biofuels (Haynes and Gonzalez, 2014), and allow for the omission of an oxygen input requirement if applied industrially.

In recent years, hyperthermophilic archaea such as the *Thermococcus spp.* and *Pyrococcus spp.* have been developed as metabolic hosts for producing fuels and commodities. These include the production of hydrogen (Lipscomb et al., 2014), 3-hydroxypropionate (Keller et al., 2013), and butanol (Keller et al., 2015) in *Pyrococcus furiosus* (Zeldes et al., 2015) as well as the production of hydrogen from carbon monoxide in *Thermococcus onnurineus* via adaptive evolution (Lee et al., 2016). Regarding methanogens (note all known methanogens are anaerobic archaea), *Methanococcus maripaludis* has been recently engineered to produce geraniol during autotrophic growth via expression of a single heterologous gene (Lyu et al., 2016), and *M. acetivorans* was engineered to use the industrial solvents methyl acetate and methyl propionate as carbon sources by cloning *mekB* from *Pseudomonas veronii* (Lessner et al., 2010). Here, we metabolically engineered *M. acetivorans* to produce optically pure *L*-lactic acid from methane. This is the first report of metabolic engineering of a methanogen using a biosynthetic pathway.

Results and Discussion

Design of the Metabolic Pathway for Butanol Production From Methane

With the production of acetate from methane (Soo et al., 2016), we reasoned we could convert the intermediate for acetate, acetyl-CoA, into butanol (Fig. 1) based on the pathway demonstrated in metabolically-engineered *E. coli* (Shen et al., 2011). Using *M. acetivorans* as the host, we intended to synthesize butanol from the production of Mcr from ANME-1, from the production of Crt, Hbd, and AdhE2 from *C. acetobutylicum*, and from the production of Ter from *T. denticola*. Instead of including AtoB from *E. coli* in the butanol production pathway, the native acetyl-CoA acetyltransferase, MA_4042, from the *M. acetivorans* host was used since we reasoned it was more likely to be active in the archaeon.

Optimization of Transformation

We had difficulty transforming into *M. acetivorans* the final butanol plasmid pES1-MATbiohol-B4 (Supplementary Fig. S1) for producing McrBGA from ANME-1, for producing AdhE2, Crt, and Hbd from *C. acetobutylicum*, for producing Ter from *T. denticola*, and for producing MA_4042 from *M. acetivorans* (Fig. 1); therefore, we optimized the HS methanol medium for growth to improve the transformation of large plasmids. We tried increasing the methanol concentration (75, 125, 185, 250, and 500 mM) and tried adding yeast extract (2.5, 5, 10, and 15 g/L), since the addition of yeast extract or casamino acids to the growth medium was originally described as slightly stimulatory for growing *M. acetivorans* (Sowers et al., 1984). We found that adding yeast extract at the lowest concentration (2.5 g/L) decreased the lag phase (Fig. 2A) whereas increasing methanol increased the lag phase (Fig. 2B). Therefore,

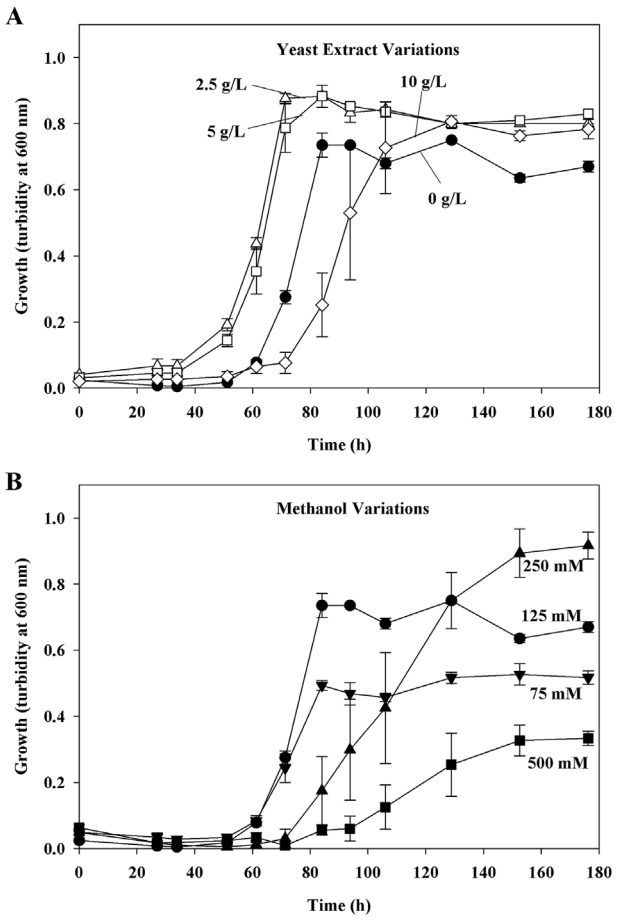

Fig. 2. Growth curves for optimization of medium for *M. acetivorans*. Cultures were grown in HS medium at 37°C (**A**) having methanol concentration fixed at 125 mM and with the addition of varied amounts of yeast extract (2.5 g/L Δ, 5 g/L □, or 10 g/L ◇), or (**B**) having varied amounts of methanol concentrations (75 mM ▼, 125 mM ●, 250 mM ▲, or 500 mM ■) without yeast extract. Three independent cultures were tested for each condition, and error bars represent standard errors of the means.

yeast extract at 2.5 g/L was included, while the methanol concentration was kept at 125 mM, to make HSYE medium, which was used for subsequent culturing and transformations. Using HSYE medium led to successful transformation, while the use of HS medium led to no successful transformations after eight attempts.

Producing McrBGA, MA_4042, AdhE2, Ter, Crt, and Hbd Leads to the Formation of Lactate From Methane

When *M. acetivorans* containing the plasmid pES1-MATbiohol-B4 (containing genes for producing Ter, Crt, Hbd, McrBGA, MA_4042, and AdhE2, Supplementary Fig. S1) was tested with methane in a high cell-density experiment (Soo et al., 2016), significant amounts of butanol formation were not detected. However, in comparison to *M. acetivorans* containing either plasmid pES1-MAT*mcr3* (containing genes for producing McrBGA) or pES1-MATbiohol-B3 (an intermediate plasmid used in constructing pES1-MATbiohol-B4 containing genes for producing McrBGA, MA_4042, and AdhE2, Supplementary Fig. S1), acetate production amounts decreased by 12.4-fold (Fig. 3A), methane consumption amounts remained similar (Fig. 3A), and an additional peak was seen in high-performance liquid chromatography (HPLC) chromatograms (Fig. 4) of supernatants from *M. acetivorans* containing plasmid

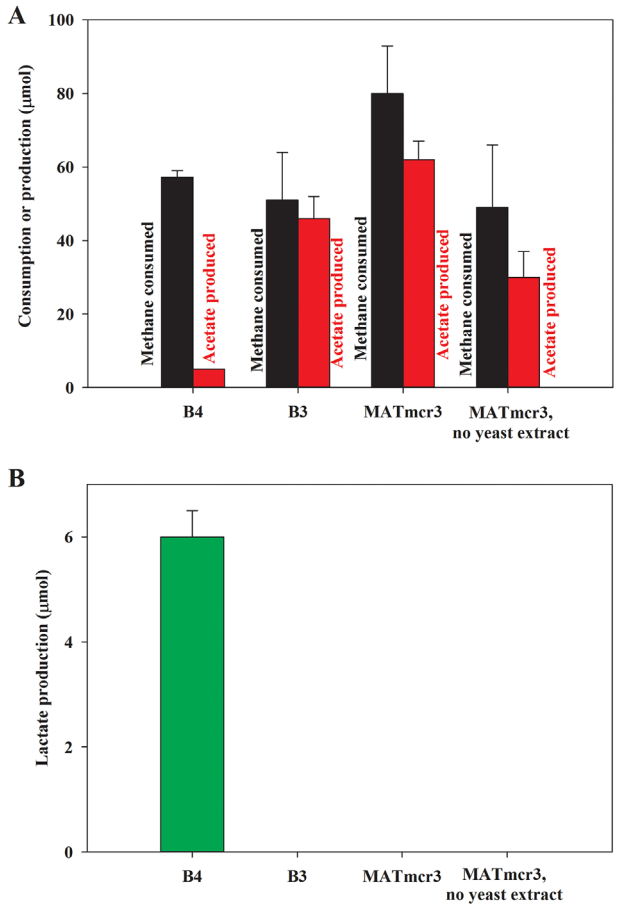

Fig. 3. Consumption of methane, and production of acetate and lactate by ANME-1 Mcr-producing strains of *M. acetivorans* during high-density growth experiments. Methane consumption (**A**) and lactate production (**B**) of cells harboring pES1-MATbiohol-B4 (B4, contains *mcrBGA*, *ma_4042*, *adhE2*, *ter*, *crt*, and *hbd*), pES1-MATbiohol-B3 (B3, contains *mcrBGA*, *ma_4042*, and *adhE2*), and pES1-MAT*mcr3* (MATmcr3, contains *mcrBGA*) after 5 days. All strains were tested with 2.5 g/L yeast extract unless otherwise indicated. Three independent cultures were tested for each condition, and error bars represent one standard deviation.

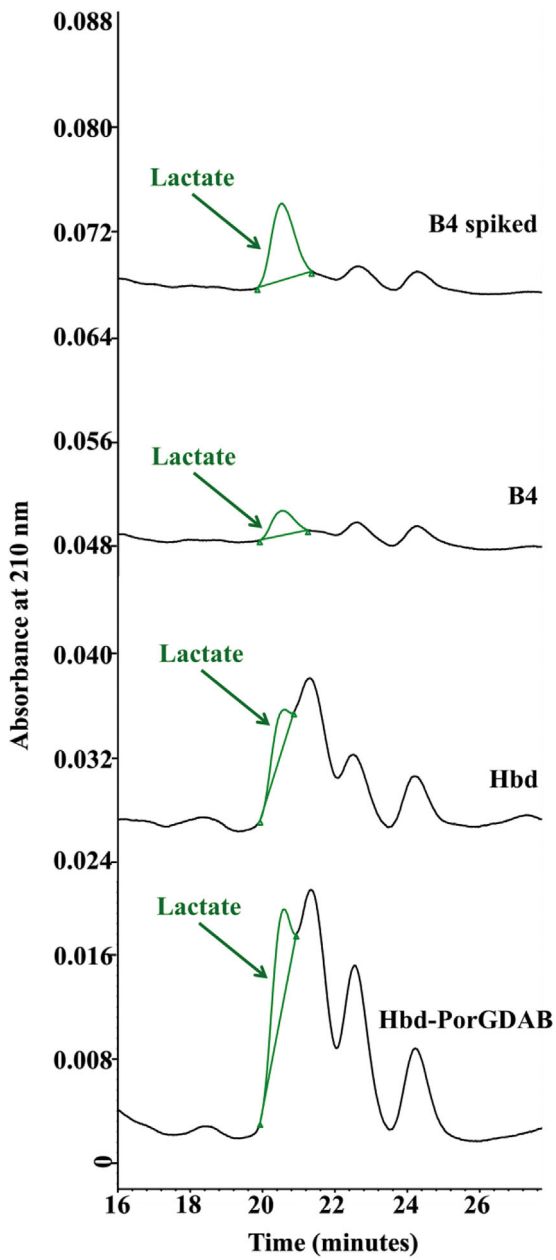

Fig. 4. HPLC chromatograms of cultures producing lactate. Chromatogram of cells harboring pES1-MATbiohol-B4 (B4) consuming methane for 5 days showing a lactate peak (green, labeled). The same sample had the equivalent of 2 mM lactate added to confirm the peak under question belonged to lactate (B4 spiked). Chromatograms of cells harboring pES1-MAT*mcr3-hbd* (Hbd) or pES1-MAT*mcr3-hbd-porGDAB* (Hbd-Por) that were grown in HSYE with 125 mM methanol for 27 days. All chromatograms shown here are focused on the lactate peak (displayed in green), with lactate having a retention time of 20.5 min.

pES1-MATbiohol-B4. This indicated that acetate (previously shown to originate from methane (Soo et al., 2016)) was further converted into another secreted by-product. By testing for various alcohols and acids (methanol, ethanol, acetoacetatic acid, 3-hydroxybutyric acid, crotonic acid, butyraldehyde, fumaric acid, succinic acid, and lactic acid), this product was identified as lactate by HPLC (Figs. 3 and 4B) and by liquid chromatography-mass spectrometry (LC-MS); the lactate produced has a m/z ratio of 89.05, closely matching 89.03 as previously determined (Ibanez and Bauer, 2014) (Supplementary Fig. S2). The yield from the metabolically-engineered strain was 0.105 ± 0.009 mol lactate/mol methane (corresponding to 0.59 ± 0.05 g lactate/g methane), and the lactate was secreted, with sonication of the samples showing a negligible increase in lactate concentrations by 1.3 ± 0.2 fold.

The inclusion of yeast extract during the 5-day incubation period under methane did not significantly affect the acetate yield for the host containing the plasmid pES1-MAT*mcr*3 (0.61 ± 0.26 μmol acetate/μmol methane consumed without yeast extract, compared to 0.78 ± 0.14 μmol acetate/μmol methane consumed with yeast extract). In addition, incubating the pES1-MATbiohol-B4 host under a nitrogen headspace (compared to a methane headspace) in a high cell density experiment that includes yeast extract led to a 9 ± 3 fold decrease in lactate production (5.3 ± 0.6 μmol vs. 0.6 ± 0.2 μmol); no lactate was detected in the three replicates which lacked cells but included methane and yeast extract in the medium. Thus, the lactate produced with pES1-MATbiohol-B4 did not originate from yeast extract and is derived from methane. Also, lactate was not produced by the host transformed with pES1-MAT*mcr*3 (which produces only Mcr) (Fig. 3B) so production of Mcr alone only allows for production of acetate, and is not sufficient to produce lactate.

Stereochemistry of the Produced Lactate

In order for the produced lactate to be suitable as a substrate for polylactic acid synthesis, optical purity is required (Bogaert and Coszach, 2000). Therefore, we determined which lactate stereospecific isomer was produced by the host containing the pES1-MATbiohol-B4 plasmid using kits specific for detecting *D*-lactate (MAK058-1KT, Sigma–Aldrich, St. Louis, MO) and *L*-lactate (MAK065-1KT, Sigma–Aldrich): 1.1 ± 0.2 mM of *L*-lactate was produced, while no *D*-lactate was found in the samples. Furthermore, the concentration of lactate found by the kit was corroborated by assaying lactate concentrations via HPLC (1.2 ± 0.1 mM corresponding to 6.0 ± 0.5 μmol) (Fig. 4).

Hbd Produces Lactate From Acetate in *M. acetivorans*

We reasoned that Hbd was responsible for the lactate produced from the methane that was converted to acetate by Mcr using plasmid pES1-MATbiohol-B4 since no lactate production occurred with the host containing pES1-MATbiohol-B3 (produces McrBGA, MA_4042, and AdhE2, Fig. 3B), so MA_4042 and AdhE2 were not responsible for lactate production. The most direct path for lactate production from methane (Fig. 1) involves a lactate dehydrogenase to modify the ketone group in pyruvate to a hydroxyl group, yielding lactate. Out of Ter, Crt, and Hbd,

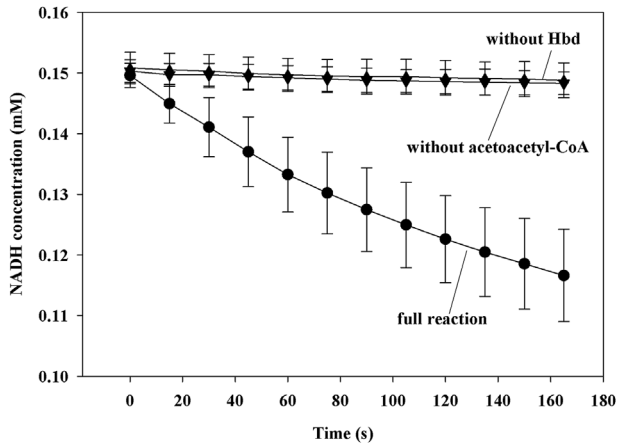

Fig. 5. Enzymatic assays performed in vitro using Hbd purified from an *E. coli* host. Enzyme assays for the positive control reaction (acetoacetyl-CoA + NADH → 3-hydroxybutyryl-CoA + NAD^+). The positive control reactions (●) included 1 μg/mL Hbd protein. Negative control reactions omitted either Hbd (▼) or the acetoacetyl-CoA substrate (▲). NADH concentrations were determined by monitoring A_{340}, and two reactions were tested for each condition with error bars representing one standard deviation.

Hbd is the only enzyme that converts a ketone group to a hydroxyl group. To investigate whether Hbd is responsible for lactate production, we performed in vitro assays with purified Hbd produced from *E. coli*. These assays indicated no lactate dehydrogenase activity in the direction of lactate production (using pyruvate as substrate), even though the purified enzyme was active with regard to its known 3-hydroxybutyryl-CoA dehydrogenase activity with acetoacetyl-CoA as substrate (Guterl et al., 2012; Sommer et al., 2013) (Fig. 5). Also, no lactate production was seen in vivo with *E. coli* producing Ter, Crt, or Hbd (from pET27b-Pfer-*ter*, pET27b-Pfer-*crt*, and pET27b-Pfer-*hbd*; plasmid maps shown in Supplementary Fig. S3) (results not shown).

Since assays using enzymes produced by *E. coli* failed to demonstrate which of the enzymes Ter, Crt, or Hbd were responsible for lactate production, further assays were performed with the *M. acetivorans* host by using plasmids in which Ter, Crt, or Hbd of the original pES1-MATbiohol-B4 plasmid were produced individually (along with Mcr). Hence, we transformed *M. acetivorans* with plasmids pES1-MAT*mcr*3-Pfer-*ter*, pES1-MAT*mcr*3-Pfer-*crt*, and pES1-MAT*mcr*3-Pfer-*hbd* (Supplementary Fig. S1). We also tested a construct in which Por (pyruvate ferredoxin oxidoreductase) from *M. acetivorans* was added with Hbd (along with Mcr) in pES1-MAT*mcr*3-Pfer-*hbd-porGDAB*. Por catalyzes the interconversion between acetyl-CoA and pyruvate (Fig. 1), principally in the direction of pyruvate synthesis in vivo (Santiago-Martinez et al., 2016), so Por was included in the hopes of increasing lactate production. Analyzing the transformants grown in HSYE with 125 mM methanol by HPLC revealed the production of lactate only in cells producing Hbd (pES1-MAT*mcr*3-Pfer-*hbd*, pES1-MAT*mcr*3-Pfer-*hbd-por*GDAB, and pES1-MATbiohol-B4; Figs. 4 and 6). Significant lactate dehydrogenase activity in the direction of lactate formation was also detected from

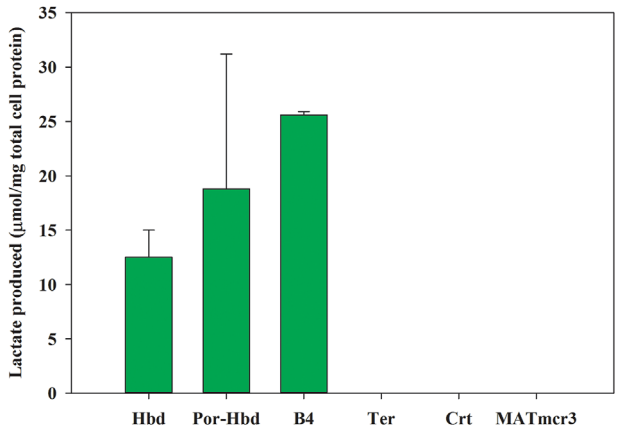

Fig. 6. Production of lactate from methanol. *M. acetivorans* harboring pES1-MAT*mcr*3-Pfer-*hbd* (Hbd), pES1-MAT*mcr*3-Pfer-*hbd-porGDAB* (Hbd-Por), pES1-MAT-biohol-B4 (B4), pES1-MAT*mcr*3-Pfer-*ter*, pES1-MAT*mcr*3-Pfer-*crt*, and, and pES1-MAT*mcr*3 (MATmcr3). Cultures were grown in HSYE medium with 125 mM methanol at 37°C for between 16 and 51 days. Two independent cultures were tested for each strain, and error bars represent one standard deviation.

total cell lysates of *M. acetivorans* hosting pES1-MAT*mcr*3-Pfer-*hbd*, and not from cells hosting pES1-MAT*mcr*3 (Supplementary Fig. S4). Hence, Hbd is active in *M. acetivorans* and is used to produce lactate (Fig. 1). However, the additional production of Por alongside Hbd and Mcr, compared to Hbd and Mcr alone, did not significantly increase lactate production (Fig. 6).

Conclusions

We demonstrate here successful metabolic engineering of an archaeon host to produce and secrete optically pure *L*-lactate from methane anaerobically. Furthermore, the yield of 0.59 g lactate/g methane is 10 fold greater than that reported for the aerobic conversion of methane to lactate (0.050 g lactate/g methane [Henard et al., 2016]), and the volumetric lactate production rate in our 5-mL culture size (0.00090 ± 0.00008 g lactate/L/h) is comparable to that in a 300-mL culture of the aerobic process (Henard et al., 2016) . We also show the biochemistry of the process for methane conversion to lactate involves Hbd from *C. acetobutylicum.* Hbd likely converts pyruvate to lactate; hence, Hbd from *C. acetobutylicum* is active in *M. acetivorans*. Hbd produced from *E. coli* does not display the desired lactate production activity, so we hypothesize that post-translational modifications from the *M. acetivorans* host changes the substrate specificity of Hbd from acetoacetyl-CoA to pyruvate. While significant optimization is required to increase methane consumption and overall yield of lactate to make an economically competitive process, this work represents a proof of concept that methane can be converted to another value-added product in an anaerobic process.

Methods

Reagents, Bacterial Strains, and Cultivation Conditions

The *M. acetivorans* strains (Table I) were routinely grown anaerobically as pre-cultures at 37°C in an 80% N_2/19% CO_2/1% H_2 atmosphere with mild shaking in 10 mL HS medium (Metcalf et al., 1996) or HSYE (HS medium with 2.5 g/L yeast extract) with 125 mM methanol as the carbon source, unless otherwise indicated. All 28-mL culture tubes (18 × 150 mm, Bellco Glass, Vineland, NJ) were sealed by aluminum crimp seals and petroleum jelly was added to rubber stopper surfaces to prevent leaks. pES1-based plasmids were maintained in *M. acetivorans* with 2 μg/mL puromycin. *E. coli* HST08 (Clontech Laboratories Inc., Mountain View, CA) and *E. coli* DH5α (λpir) were used to construct plasmids before transforming into the *M. acetivorans* host. For *E. coli*, kanamycin (50 μg/mL) was used to maintain the recombinant pET27b-based plasmids, carbenicillin (100 μg/mL) was used for the recombinant pES1-based plasmids, and chloramphenicol was used (34 μg/mL) for the Rosetta (DE3) plasmid pLacI (Novagen/EMD Millipore, Billerica, MA). *E. coli* was cultured in lysogeny broth (LB) (Sambrook J and Maniatis, 1989) at 37°C with shaking at 250 rpm.

Experiments for short-duration (ca., 5 days) growth on methane, in which high cell-density inocula were used, were done as previously described (Soo et al., 2016) with modifications; 2 mL of each *M. acetivorans* strain was pre-grown in 200 mL of HS medium with 125 mM methanol (and 2 μg/mL puromycin when plasmids were present) and 2.5 g/L yeast extract at 37°C for 5 days (turbidity at 600 nm ∼1.0). Cells were collected by centrifugation (5,000 rpm for 20 min), and were washed three times with HS medium and puromycin alone to remove residual methanol. The final cell pellet was resuspended using 5 mL of HS medium supplemented with 10 mM $FeCl_3$ and 2 μg/mL puromycin, with 2.5 g/L yeast extract unless otherwise indicated, to yield a density of 4×10^{10} CFU/mL. The headspace of each tube was replaced with 950 μmol of methane (or nitrogen where indicated). The tubes were then incubated at 37°C with shaking at 250 rpm for 5 days.

Optimization of growth was performed by growing *M. acetivorans* in HS medium with varied concentrations of methanol (75, 125, 185, 250, and 500 mM) and yeast extract (2.5, 5, 10, and 15 g/L) (Sowers et al., 1984). Cells were inoculated at an initial turbidity of 0.05 at 600 nm, incubated at 37°C, and growth was monitored via turbidity at 600 nm.

Transformation of *M. acetivorans*

All plasmids were transformed into *M. acetivorans* using a liposome-mediated procedure (Metcalf et al., 1997) with slight modifications. Cells (2 mL) grown in HSYE with 125 mM methanol to a turbidity at 600 nm of 0.2–0.5 were centrifuged and resuspended into 1 mL of 850 mM sucrose and 80 mM sodium bicarbonate (pH 7.4). DNA: liposome complexes were made by mixing plasmid DNA (4–6 μg) with 15–25 μL of DOTAP (n-(1-(2,3-dioleoyloxy)propyl)-n,n,n-trimethylammonium methyl-sulfate, Sigma–Aldrich) prepared in 850 mM sucrose and 80 mM sodium bicarbonate (pH 7.4) to make a final reaction volume of 50 μL and incubated at 37°C for at least 15 min. The 1 mL cell resuspension was added to the 50 μL DNA: liposome complex and incubated at 37°C for 4 h. The cells were then transferred to 10 mL HSYE medium with 125 mM methanol, grown for 48 h, then 1 mL of the culture was added to 10 mL selective HSYE medium with 125 mM methanol and 2 μg/mL puromycin.

Table I. Strains and plasmids used in this study.

Strain/plasmid	Description	Source
M. acetivorans C2A	Wildtype *M. acetivorans*	J. G. Ferry
E. coli DH5α (λ pir)	F^- *endA1 glnV44 thi-1 recA1 relA1 gyrA96 deoR nupG* ϕ80d*lacZ*ΔM15 Δ(*lacZYA-argF*)*U169 hsdR17*($r_K^- m_K^+$) λ*pir*	W. W. Metcalf
E. coli HST08	F^- *endA*1 *supE*44 *thi*-1 *recA*1 *relA*1 *gyrA*96, *phoA,* ϕ80d*lacZ*ΔM15 Δ(*lacZYA-argF)U169* Δ(*mrr-hsdRMS-mcrBC*) Δ*mcrA,* λ^-	Clontech
E. coli Rosetta™ DE3	F^- *ompT hsdS*$_B$($r_B^- m_B^-$) *gal dcm* (DE3)	Novagen
placI	Cam^R, p15A *ori*, *lacI*, *ileX*, *argU*, *thrU*, *tyrU*, *glyT*, *thrT*, *argW*, *metT*, *leuW*, *proL*	Novagen
pES1(Pmat)	Amp^R, Pur^R, R6K *ori*, C2A *ori*, $P_{mcr\_ANME\text{-}1}$	Soo et al. (2016)
pES1(PmatSpeI)	Amp^R, Pur^R, R6K *ori*, C2A *ori*, *SpeI*::$P_{mcr\_ANME\text{-}1}$	This study
pES1-MAT*mcr*3	Amp^R, Pur^R, R6K *ori*, C2A *ori*, $P_{mcr\_ANME\text{-}1}$::$mcr_{ANME\text{-}1}$	Soo et al. (2016)
pES1-PmatSpeI-*ma_4042-adhE2*	Amp^R, Pur^R, R6K *ori*, C2A *ori*, *SpeI*::$P_{mcr\_ANME\text{-}1}$ ::*ma_4042*::*adhE2*	This study
pES1-PmatSpeI-*ter-crt-hbd*	Amp^R, Pur^R, R6K *ori*, C2A *ori*, *SpeI*::$P_{mcr\_ANME\text{-}1}$::*ter*::*crt*::*hbd*	This study
pES1-MATbiohol-B3	Amp^R, Pur^R, R6K *ori*, C2A *ori*, $P_{mcr\_ANME\text{-}1}$::$mcr_{ANME\text{-}1}$::$P_{mcr\_ANME\text{-}1}$::*ma_4042*::*adhE2*	This study
pES1-MATbiohol-B4	Amp^R, Pur^R, R6K *ori*, C2A *ori*, $P_{mcr\_ANME\text{-}1}$::$mcr_{ANME\text{-}1}$::$P_{mcr\_ANME\text{-}1}$ ::*ma_4042*::*adhE2*::$P_{mcr\_ANME\text{-}1}$::*ter*::*crt*::*hbd*	This study
pET27b	Km^r, pBR322 ori, P_{T7}	Novagen
pET27b-*hbd*HisC	Km^r, pBR322 ori, P_{T7}::*hbd*::his_6	This study
pET27b-Pfer-*hbd*	Km^r, pBR322 ori, P_{T7}::P_{fer}::*hbd*	This study
pES1-MAT*mcr*3-Pfer-*hbd*	Amp^R, Pur^R, R6K *ori*, C2A *ori*, $P_{mcr\_ANME\text{-}1}$::$mcr_{ANME\text{-}1}$::P_{fer}::*hbd*	This study
pET27b-Pfer-*crt*	Km^r, pBR322 ori, P_{T7}::P_{fer}::*crt*	This study
pES1-MAT*mcr*3-Pfer-*crt*	Amp^R, Pur^R, R6K *ori*, C2A *ori*, $P_{mcr\_ANME\text{-}1}$::$mcr_{ANME\text{-}1}$::P_{fer}::*crt*	This study
pET27b-Pfer-*ter*	Km^r, pBR322 ori, P_{T7}::P_{fer}::*ter*	This study
pES1-MAT*mcr*3-Pfer-*ter*	Amp^R, Pur^R, R6K *ori*, C2A *ori*, $P_{mcr\_ANME\text{-}1}$::$mcr_{ANME\text{-}1}$::P_{fer}::*ter*	This study
pET27b-Pfer-*hbd-porGDAB*	Km^r, pBR322 ori, P_{T7}::P_{fer}::*hbd*::*porGDAB*	This study
pES1-MAT*mcr*3-Pfer-*hbd-porGDAB*	Amp^R, Pur^R, R6K *ori*, C2A *ori*, $P_{mcr\_ANME\text{-}1}$::$mcr_{ANME\text{-}1}$::P_{fer}::*hbd*::*porGDAB*	This study

Cloning of Genes for Butanol Formation

The In-Fusion™ cloning technique (Clontech) was used to clone each of the amplified fragments unless otherwise stated. Oligonucleotide sequences used for amplifying the desired enzyme gene sequences are given in Supplementary Table SI. The sequences of all the plasmids used in this work are available in the FASTA format in the Supplementary Data 1.

Before cloning the genes encoding the enzymes AdhE2, Ter, Crt, and Hbd into the pES1-based vector, the vector pES1(Pmat) (Soo et al., 2016) had to be modified to include an SpeI site just upstream of the $P_{mcr\_ANME\text{-}1}$ promoter to create pES1(PmatSpeI) (Supplementary Fig. S1); SpeI is one of the few enzymes that does not cut pES1(Pmat) or cut the *ma_4042*::*adhE2* or *ter*, *crt*, and *hbd* inserts. To construct pES1(PmatSpeI), the $P_{mcr\_ANME\text{-}1}$ promoter from the metagenome of a microbial mat found in the Black Sea (Shima et al., 2012) was used since it is activated by methane (Soo et al., 2016). $P_{mcr\_ANME\text{-}1}$ was amplified from pES1(Pmat) via pES1PmatSpeI-f and MATmcr-r, then both insert and vector pES1(Pmat) were digested with KpnI and NheI restriction enzymes. The KpnI/NheI digest of pES1(Pmat) was treated with alkaline phosphatase to remove phosphate groups from the 5′ ends to prevent re-ligation. The digested promoter insert was ligated into the treated vector with T4 DNA ligase, and the SpeI::$P_{mcr\_ANME\text{-}1}$ section of the plasmid was confirmed by sequencing using primer veri-p-f (Supplementary Table SI).

The non-*M. acetivorans* genes *adhE2*, *ter*, *crt*, and *hbd* were designed with SpeI and NheI restriction sites and were codon optimized using GENEius (at http://www.geneius.de/GENEius/Orf_start.action) and the codon optimization table of *M. acetivorans* from the CUTG database (Nakamura et al., 2000), while avoiding potential secondary structures. The designed fragments (two 1000-bp fragments and one 750-bp fragment that yield *adhE2* when combined, and three 1000-bp fragments that yield the ter::crt::hbd segment when combined) were synthesized by Eurofins MWG Operon LLC (Louisville, KY). The gene *ma_4042* that originates from the *M. acetivorans* host was amplified from the genome using the primers ma_4042-mat-f and ma_4042-r (Table I) as a 1251 bp fragment. The three fragments containing portions of *adhE2* were amplified using primers adhE2-1f and adhE2-1r, adhE2-2f and adhE2-2r, and adhE2-3f and MATmcr-r (Supplementary Table SI). Then, the three *adhE2* fragments, the *ma_4042* fragment, and pES1 (PmatSpeI) (cut by NheI and treated with FastAP phosphatase to remove phosphate groups on the 5′ ends to prevent re-ligation) were joined together via the Gibson assembly method (Gibson et al., 2009) to construct the intermediate plasmid pES1-PmatSpeI-*ma_4042-adhE2* (Supplementary Fig. S1), with the entire SpeI::$P_{mcr\_ANME\text{-}1}$::*ma_4042*::*adhE2* section confirmed by sequencing using primers veri-p-f, MATmcr-r, ma_4042-r, adhE2-1r, adhE2-2r, and adhE2-3f (Supplementary Table SI). The intermediate vector pES1-PmatSpeI-ter-crt-hbd (Supplementary Fig. S1) was constructed in a similar fashion. The synthesized *ter*, *crt*, and *hbd* fragments were amplified using the primers Gene-Pmat-f and ter-1r, ter-crt-f and ter-crt-r, and crt-hbd-f and MATmcr-r (Supplementary Table SI), respectively. The vector pES1(PmatSpeI) was cut by restriction enzyme NheI, and the cut vector and amplified *ter*, *crt*, and *hbd* fragments were joined together via the Gibson assembly method (Gibson et al., 2009) to construct pES1-PmatSpeI-*ter-crt-hbd*, with the entire SpeI::$P_{mcr\_ANME\text{-}1}$::*ter*::*crt*::*hbd* section confirmed by sequencing using the primers veri-p-f, but4-f4, ter-crt-r, but4-f5, and pES1-r (Supplementary Table SI).

The intermediate butanol production plasmid pES1-MATbiohol-B3 (Supplementary Fig. S1) lacking *ter*, *crt*, and *hbd*, was constructed by digesting pES1-PmatSpeI-*ma_4042-adhE2* with SpeI and NheI, digesting pES1-MAT*mcr*3 with NheI, and dephosphorylating, then ligating the obtained *ma_4042*::*adhE2* fragment and the cut/dephosphorylated pES1-MAT*mcr*3. The entire $P_{mcr\_ANME\text{-}1}$::*ma_4042*::*adhE2* segment of pES1-MATbiohol-B3 was confirmed by sequencing using primers primers B6-f, biohol-B1-1f, adhE2-1f, ma_4042-r, biohol-B1-2f, adhE2-2f, adhE2-3f, and MATmcr-r (Supplementary Table SI).

The final plasmid for supposed butanol production, pES1-MATbiohol-B4 (Supplementary Fig. S1), was constructed by digesting pES1-PmatSpeI-*ter-crt-hbd* with SpeI and NheI, then ligating the SpeI::$P_{mcr\_ANME\text{-}1}$::*ter*::*crt*::*hbd* fragment into an NheI-cut and dephosphorylated pES1-MAT*mcr*3-*ma_4042-adhE2*; the entire $P_{mcr\_ANME\text{-}1}$::*ma_4042*::*adhE2*::$P_{mcr\_ANME\text{-}1}$::*ter*::*crt*::*hbd* segment was confirmed using primers E1-seq1-f, butf-f6, biohol-B1-1f, but4-f1, butf-f2, adhE2-3f, but4-f3, but4-f4, ter-crt-r, but4-f5, and pES1-r (Supplementary Table SI).

Cloning of *hbd, crt, ter,* and *hbd-porGDAB* Genes into pES1-MAT*mcr*3

The production of three enzymes (Hbd, Crt, and Ter) from pES1-MATbiohol-B4 by *M. acetivorans* unexpectedly led to production of lactate. To determine which enzyme was responsible for producing lactate, we cloned the genes encoding the respective enzymes (*hbd*, *crt*, *ter*, and *hbd-porGDAB*) into *M. acetivorans* downstream of a ferredoxin promoter (P_{fer}) (that displayed increased transcription under methane (Soo et al., 2016)) into pES1-MATmcr3 downstream of the *mcrBGA* genes. The genes *hbd*, *crt*, and *ter* were amplified from pES1-MATbiohol-B4 as the template, and the P_{fer} promoter was amplified from genomic DNA of *M. acetivorans* C2A.

Because of the difficulty in the cloning of these fragments, P_{fer}::*hbd*, P_{fer}::*crt*, P_{fer}::*ter*, and P_{fer}::*hbd*::*porGDAB* into a large vector (pES-1MAT*mcr*3, 14,348 bases) in a single reaction with the In-Fusion™ cloning technique, cloning was split into two steps. The first step consisted of cloning two fragments, whereby each fragment was amplified using respectively designed primers (*hbd*, *crt*, and *ter* fragments were amplified using primers hbd-f and pET27b-hbd-r, crt-f and pET27b-crt-r, and ter-f and pET27b-ter-r, respectively; Supplementary Table SI), then the P_{fer} fragment (amplified using pET27b-Pfer-f paired with Pfer-hbd-r, Pfer-crt-r, or Pfer-ter-r; Supplementary Table SI) was fused to each protein-coding gene (*hbd*, *crt*, and *ter*, respectively). Each subsequent fragment was cloned into the pET27b vector between the *Nde*I and *Xho*I sites, and transformed into the propagation host *E. coli* HST08. Each fragment that successfully fused the gene to the P_{fer} promoter (segments P_{fer}::*hbd*, P_{fer}::*crt*, and P_{fer}::*ter* in pET27b-Pfer-*hbd*, pET27b-Pfer-*crt*, and pET27b-Pfer-*ter* as in Supplementary Fig. S3, respectively) was confirmed by sequencing using primers T7-f and T7-r (Supplementary Table SI) and were individually inserted into the NheI site of pES1-MAT*mcr*3 via In-Fusion™ cloning, and electroporated into the host *E. coli* DH5α (λ pir). The segments P_{fer}::*hbd*, P_{fer}::*crt*, and P_{fer}::*ter* in the resulting plasmids pES1-MAT*mcr*3-Pfer-*hbd*, pES1-MAT*mcr*3-Pfer-*crt*, and pES1-MAT*mcr*3-Pfer-*ter* (Supplementary Fig. S1), respectively, were confirmed by sequencing using primers SC-f and SC-r (Supplementary Table SI) and transformed into the *M. acetivorans* for the estimation of lactate production.

Cloning of *porGDAB* into pES1-MAT*mcr*3-Pfer-*hbd*

In a similar fashion, the *porGDAB* operon was amplified from genomic DNA of *M. acetivorans* C2A using the primers porG-27b-f and porB-27b-r (Table I), then inserted into the NheI site of pET27b-Pfer-*hbd* using the Gibson assembly method (Gibson et al., 2009) to construct the intermediate plasmid pET27b-Pfer-*hbd-porGDAB* (Supplementary Fig. S3). The P_{fer}::*hbd*::*porGDAB* fragment was then excised using XbaI and NheI restriction enzymes, and inserted into the NheI site of pES1-MAT*mcr*3 to generate the final plasmid pES1-MAT*mcr*3-Pfer-*hbd-porGDAB* (Supplementary Fig. S3), with the entire P_{fer}::*hbd*::*porGDAB* segment confirmed by sequencing using the primers SC-f, porG-27b-f, porD-f, porA-r, and porB-r2 (Supplementary Table SI).

Cloning, Expression, and Purification of HbdHisC

We cloned, expressed, and purified 3-hydroxybutyryl-CoA dehydrogenase (Hbd) with a His_6 tag fused to the C-terminus with a short linker (GSG) in *E. coli* to perform in vitro assays for the production of lactate from pyruvate. Using the pES1-MATbiohol-B4 plasmid as the template, *hbd* was amplified using the primers hbd-HisC-f and hbd-HisC-r (Supplementary Table SI), and cloned into the pET27b vector between the *Nde*I and *Xho*I sites. The resulting pET27b-*hbd*HisC plasmid (Supplementary Table SI) was confirmed by sequencing from the ribosome binding site to the end of the his_6 tag using primers T7-f and T7-r (Supplementary Table SI).

A positive clone was transformed into expression host *E. coli* Rosetta (DE3) pLacI, cultured in 1 L of LB medium until the turbidity at 600 nm reached 0.8, and Hbd was produced by adding isopropyl-β-D-thiogalactopyranoside (IPTG, 1 mM). After Hbd production for 20 h at 25°C, cells were chilled for 10 min, centrifuged, and the pellet was suspended in 20 mL of loading buffer (20 mM sodium phosphate, 500 mM NaCl, 20 mM imidazole, pH 7.4) which was supplemented with 200 μg/mL lysozyme (Sigma–Aldrich) and 100 μL of protease inhibitor cocktail (Sigma–Aldrich), and incubated on ice for 30 min. Sonication (Qsonica, LLC, Model Q700, Newtown, CT) was performed six times for 30 s at amplitude 45%. The lysate was centrifuged at 18,000*g* for 20 min, and the cytoplasmic fraction (supernatant) was loaded onto a 5 mL HisTrap™ FF column (GE Healthcare, Piscataway, NJ) which was pre-equilibrated with 10 column volumes of wash buffer (20 mM sodium phosphate, 500 mM NaCl, 40 mM imidazole, pH 7.4), followed by 10 column volumes of wash buffer, and the bound protein was eluted using a 10 min linear imidazole gradient in elution buffer (20 mM sodium phosphate, 500 mM NaCl, 250 mM imidazole, pH 7.4). The eluted protein (HbdHisC) was analyzed by SDS–PAGE (Supplementary Fig. S4) and the purified protein fractions were pooled and concentrations were estimated by Bradford method using BSA as standard. The buffer of the purified protein HbdHisC was exchanged to 50 mM HEPES, pH 7.0.

Enzymatic Activity Assays Performed In Vitro

Enzymatic activity of purified Hbd from *E. coli* was tested in vitro aerobically as indicated by Sommer et al. (2013) with modifications. Assays were performed in reaction mixtures in 50 mM HEPES at pH 7, with 0.15 mM acetoacetyl-CoA or sodium pyruvate, and 0.15 mM NADH at 37°C. Reactions were started by the addition of 1 or 10 μg/mL purified Hbd, or 100 μg/mL total cell protein from *M. acetivorans* containing pES1-MAT*mcr*3-Pfer-*hbd* or pES1-MAT*mcr*3, and the progress of the reaction was assayed by monitoring NADH concentrations via the absorbance change at 340 nm. Enzymatic activity with sodium pyruvate as the substrate was also tested in other buffers (200 mM Tris-Cl pH 7.0, 50 mM sodium acetate pH 5.2, and 50 mM Tris-Cl pH 9.0), and with varied pyruvate concentrations (0.15, 1.5, and 15 mM).

In Vivo Assays for Lactate Production From *E. coli*

Overnight cultures of the *E. coli* strains grown in LB with kanamycin (duplicate cultures per strain) were refreshed by adding 0.25 mL of the overnight into 25 mL LB with kanamycin. Cultures were then induced with 1 mM IPTG upon reaching a turbidity at 600 nm of 0.6. Samples were collected after 0, 4, and 20 h after induction, centrifuged, and pellets and supernatants were kept separately at −20°C. All supernatants were analyzed for lactate via HPLC and *D*-lactate (MAK058-1KT, Sigma–Aldrich) and *L*-lactate (MAK065-1KT, Sigma–Aldrich) kits, and cell pellets from the 4-h collection point were resuspended in 1 volume deionized water, sonicated, and analyzed by HPLC.

Gas Chromatography (GC) and HPLC

GC analyses for quantifying methane in the culture headspace were done as previously described (Soo et al., 2016). Aliquots of 100 μL volumes were injected into a 6890 N Agilent gas chromatograph equipped with a 60/80 Carboxen-1000 column (4600 × 2.1 mm, Supelco catalog no. 12390-U) and a thermal conductivity detector. The injector, column, and detector were maintained at 150°C, 180°C, and 280°C, respectively. Carrier gas flow (nitrogen) was kept at 20 mL/min, and reference gas flow (also nitrogen) for the detector at 20 mL/min as well. Gases were identified according to their retention times and their concentrations were determined according to comparisons with standards.

GC analyses for alcohols (methanol, ethanol, and n-butanol) were conducted after mixing 100 μL of a supernatant sample with 10 μL 1% vol/vol isopropanol in water as an internal reference for the injection of small liquid volumes. 1 μL of the mix was injected through the 6890 N Agilent gas chromatograph equipped with a 0.1% AT-1000 column (6′, 1/8" O.D., 80/100 mesh on Graphpac™-GC support, Alltech part no. 8542) and a flame ionization detector. The injector and detector temperatures were maintained at 150°C and 210°C, respectively, while the column temperature was maintained at 50°C for 1 min, then increased to 200°C at a rate of 50°C/min, and held at 200°C for 5 more minutes. Carrier gas flow (nitrogen) was kept at 15.4 mL/min, and gas flows of 30 mL/min hydrogen and 300 mL/min air were supplied to the detector. The alcohols that were used as standards for comparisons are methanol (EMD Millipore, catalog no. MX0485-3), ethanol (Decon Labs, King of Prussia, PA, catalog no. V1001), and n-butanol (Alfa Aesar, Ward Hill, MA, catalog no. 31068).

HPLC analyses were conducted for the detection and quantification of all organic acids under investigation (lactic acid, acetic acid, acetoacetatic acid, 3-hydroxybutyric acid, crotonic acid, butyraldehyde, fumaric acid, and succinic acid) as described previously for acetic acid (Soo et al., 2016). All supernatant samples were filtered through a 0.22 μm polyvinylidene fluoride membrane before diluting 1:6 in running buffer (0.0025 M sulfuric acid in water), then 60 μL of the 1:6 dilution was fractionated by HPLC (Waters 717 autosampler with a model 515 pump, and a 2996 photodiode array detector) with a reversed-phase column (Rezex ROA-Organic Acid H+ (8%), 300 × 7.8 mm, Phenomenex, Torrance, CA). Separations were conducted using an isocratic flow rate of 0.4 mL/min 0.0025 M sulfuric acid in water. Absorbance at 210 nm was used to detect all compounds. Chemicals used as standards for comparisons are lithium *L*-lactate (Alfa Aesar, catalog no. A11818), glacial acetic acid (EMD Millipore, catalog no. AX0073-6), lithium acetoacetate (Sigma–Aldrich, catalog no. RES1025A), 3-hydroxybutyric acid (Alfa Aesar, catalog no. 43354), crotonic acid (Fisher Scientific, catalog no. 150875000), butyraldehyde (Alfa Aesar, catalog no. A18243), sodium fumarate (Alfa Aesar, catalog no. A11276), and sodium succinate (Avantor Performance Materials, Center Valley, PA, catalog no. 7980–03). Peaks corresponding to those of lactic acid and acetic acid were confirmed by retention time, co-elution with standards, and by comparing absorbance spectra with those from the standards. Total quantities of the compounds were calculated by comparing peak areas with standard curves made by running chemical standards. LC-MS analyses were conducted as described previously (Ibanez and Bauer, 2014).

This work was supported by the Department of Energy Advanced Research Projects Agency—Energy, and T.K.W. is the Biotechnology Endowed Chair at Pennsylvania State University. The authors declare no conflict of interests. We thank James R. Miller (Penn State Proteomics and Mass Spectrometry Facility, University Park, PA) for performing the LC-MS analyses.

References

Bogaert JC, Coszach P. 2000. Poly(lactic acids): A potential solution to plastic waste dilemma. Macromol Symp 153:287–303.

Corma A, Iborra S, Velty A. 2007. Chemical routes for the transformation of biomass into chemicals. Chem Rev 107:2411–2502.

Datta R, Tsai SP, Bonsignore P, Moon SH, Frank JR. 1995. Technological and economic-potential of poly(lactic acid) and lactic-acid derivatives. FEMS Microbiol Rev 16:221–231.

Gajda I, Greenman J, Melhuish C, Ieropoulos I. 2015. Self-sustainable electricity production from algae grown in a microbial fuel cell system. Biomass Bioenerg 82:87–93.

Gao C, Ma C, Xu P. 2011. Biotechnological routes based on lactic acid production from biomass. Biotechnol Adv 29:930–939.

Gao M, Tashiro Y, Yoshida T, Zheng J, Wang QH, Sakai K, Sonomoto K. 2015. Metabolic analysis of butanol production from acetate in *Clostridium saccharoperbutylacetonicum* N1-4 using C-13 tracer experiments. Rsc Advances 5:8486–8495.

Gibson DG, Young L, Chuang RY, Venter JC, Hutchison CA, 3rd, Smith HO. 2009. Enzymatic assembly of DNA molecules up to several hundred kilobases. Nat Methods 6:343–345.

Guterl JK, Garbe D, Carsten J, Steffler F, Sommer B, Reisse S, Philipp A, Haack M, Ruhmann B, Koltermann A, Kettling U, Bruck T, Sieber V. 2012. Cell-free

metabolic engineering: Production of chemicals by minimized reaction cascades. ChemSusChem 5:2165–2172.

Haynes CA, Gonzalez R. 2014. Rethinking biological activation of methane and conversion to liquid fuels. Nat Chem Biol 10:331–339.

Henard CA, Smith H, Dowe N, Kalyuzhnaya MG, Pienkos PT, Guarnieri MT. 2016. Bioconversion of methane to lactate by an obligate methanotrophic bacterium. Sci Rep 6:21585.

Hofvendahl K, Hahn-Hagerdal B. 2000. Factors affecting the fermentative lactic acid production from renewable resources(1). Enzyme Microb Technol 26:87–107.

Hollinshead W, He L, Tang YJ. 2014. Biofuel production: An odyssey from metabolic engineering to fermentation scale-up. Front Microbiol 5:344.

Howarth RW. 2015. Methane emissions and climatic warming risk from hydraulic fracturing and shale gas development: Implications for policy. Energy Emission Control Technol 3:45–54.

Howarth RW, Santoro R, Ingraffea A. 2011. Methane and the greenhouse-gas footprint of natural gas from shale formations. Clim Change 106:679–690.

Ibanez AB, Bauer S. 2014. Analytical method for the determination of organic acids in dilute acid pretreated biomass hydrolysate by liquid chromatography-time-of-flight mass spectrometry. Biotechnol Biofuels 7:145.

Keller MW, Lipscomb GL, Loder AJ, Schut GJ, Kelly RM, Adams MW. 2015. A hybrid synthetic pathway for butanol production by a hyperthermophilic microbe. Metab Eng 27:101–106.

Keller MW, Schut GJ, Lipscomb GL, Menon AL, Iwuchukwu IJ, Leuko TT, Thorgersen MP, Nixon WJ, Hawkins AS, Kelly RM, Adams MWW. 2013. Exploiting microbial hyperthermophilicity to produce an industrial chemical, using hydrogen and carbon dioxide. Proc Natl Acad Sci USA 110:5840–5845.

Knittel K, Boetius A. 2009. Anaerobic oxidation of methane: Progress with an unknown process. Annu Rev Microbiol 63:311–334.

Lee SH, Kim MS, Lee JH, Kim TW, Bae SS, Lee SM, Jung HC, Yang TJ, Choi AR, Cho YJ, Kwon KK, Lee HS, Kang SG. 2016. Adaptive engineering of a hyperthermophilic archaeon on CO and discovering the underlying mechanism by multi-omics analysis. Sci Rep 6:22896.

Lee SY, Kim HU. 2015. Systems strategies for developing industrial microbial strains. Nat Biotechnol 33:1061–1072.

Lessner DJ, Lhu L, Wahal CS, Ferry JG. 2010. An engineered methanogenic pathway derived from the domains Bacteria and Archaea. MBio 1:e00243-10.

Lipscomb GL, Schut GJ, Thorgersen MP, Nixon WJ, Kelly RM, Adams MW. 2014. Engineering hydrogen gas production from formate in a hyperthermophile by heterologous production of an 18-subunit membrane-bound complex. J Biol Chem 289:2873–2879.

Lyu Z, Jain R, Smith P, Fetchko T, Yan Y, Whitman WB. 2016. Engineering the autotroph *Methanococcus maripaludis* for geraniol production. ACS Synth Biol 5:577–581.

Metcalf WW, Zhang J-K, Shi X, Wolfe RS. 1996. Molecular, genetic, and biochemical characterization of the serC gene of *Methanosarcina barkeri* Fusaro. J Bacteriol 178:5797–5802.

Metcalf WW, Zhang JK, Apolinario E, Sowers KR, Wolfe RS. 1997. A genetic system for Archaea of the genus *Methanosarcina*: liposome-mediated transformation and construction of shuttle vectors. Proc Natl Acad Sci USA 94:2626–2631.

Nakamura Y, Gojobori T, Ikemura T. 2000. Codon usage tabulated from international DNA sequence databases: Status for the year 2000. Nucleic Acids Res 28:292.

Reeburgh WS. 2007. Oceanic methane biogeochemistry. Chem Rev 107:486–513.

Sambrook J FE, Maniatis T. 1989. Molecular cloning: A laboratory manual. Cold Spring Harbor, N.Y.: Cold Spring Harbor Laboratory Press.

Santiago-Martinez MG, Encalada R, Lira-Silva E, Pineda E, Gallardo-Perez JC, Reyes-Garcia MA, Saavedra E, Moreno-Sanchez R, Marin-Hernandez A, Jasso-Chavez R. 2016. The nutritional status of *Methanosarcina acetivorans* regulates glycogen metabolism and gluconeogenesis and glycolysis fluxes. FEBS J 283:1979–1999.

Shen CR, Lan EI, Dekishima Y, Baez A, Cho KM, Liao JC. 2011. Driving forces enable high-titer anaerobic 1-butanol synthesis in *Escherichia coli*. Appl Environ Microbiol 77:2905–2915.

Shima S, Krueger M, Weinert T, Demmer U, Kahnt J, Thauer RK, Ermler U. 2012. Structure of a methyl-coenzyme M reductase from Black Sea mats that oxidize methane anaerobically. Nature 481:98–101.

Shindell DT, Faluvegi G, Koch DM, Schmidt GA, Unger N, Bauer SE. 2009. Improved attribution of climate forcing to emissions. Science 326:716–718.

Skjanes K, Knutsen G, Kallqvist T, Lindblad P. 2008. H2 production from marine and freshwater species of green algae during sulfur deprivation and considerations for bioreactor design. Int J Hydrogen Energy 33:511–521.

Smith WP. 1996. Epidermal and dermal effects of topical lactic acid. J Am Acad Dermatol 35:388–391.

Sommer B, Garbe D, Schrepfer P, Bruck T. 2013. Characterization of a highly thermostable beta-hydroxybutyryl CoA dehydrogenase from *Clostridium acetobutylicum* ATCC 824. J Mol Catal B: Enzym 98:138–144.

Soo VW, McAnulty MJ, Tripathi A, Zhu F, Zhang L, Hatzakis E, Smith PB, Agrawal S, Nazem-Bokaee H, Gopalakrishnan S, Salis HM, Ferry JG, Maranas CD, Patterson AD, Wood TK. 2016. Reversing methanogenesis to capture methane for liquid biofuel precursors. Microb Cell Fact 15:11.

Sowers KR, Baron SF, Ferry JG. 1984. *Methanosarcina acetivorans* sp. nov., an acetotrophic methane-producing bacterium isolated from marine sediments. Appl Environ Microbiol 47:971–978.

Upadhyaya BP, DeVeaux LC, Christopher LP. 2014. Metabolic engineering as a tool for enhanced lactic acid production. Trends Biotechnol 32:637–644.

Wee YJ, Kim JN, Ryu HW. 2006. Biotechnological production of lactic acid and its recent applications. Food Technol Biotechnol 44:163–172.

Wei H, Feng D, Pan M, Pan JY, Rao XK, Gao D. 2016. Experimental investigation on the knocking combustion characterstics of n-butanol gasoline blends in a DISI engine. Appl Energy 175:346–355.

UniProt Consortium. 2015. UniProt: A hub for protein information. Nucleic Acids Res 43:D204–D212.

Zeldes BM, Keller MW, Loder AJ, Straub CT, Adams MWW, Kelly RM. 2015. Extremely thermophilic microorganisms as metabolic engineering platforms for production of fuels and industrial chemicals. Front Microbiol 6:1209.

Supporting Information

Additional supporting information may be found in the online version of this article at the publisher's web-site.